NDVI Directionality in Boreal Forests: A Model Interpretation of Measurements

Sylvain G. Leblanc † *
Jing M. Chen †
Josef Cihlar †

Submitted to CJRS: April 21, 1997
Revised: December 16, 1997
Published: CJRS December 1997, vol. 23, pp. 368-379
Coloured figures version, November 1999.

† Canada Centre for Remote Sensing
588 Booth Street, 4th Floor
Ottawa, Canada, K1A 0Y7

* Intermap Technologies
2 Gurdwara Rd. Suite 200
Nepean, Canada, K2E 1A2

Abstract

Two-band (red and near-infrared) vegetation indices are often used in remote sensing for estimating biophysical properties of vegetated surfaces. Although many considerations have been made in formulating vegetation indices, the directionality dependency has not been comprehensively investigated. Many space-borne and air-borne remote sensing sensors acquire data in large ranges of solar and view angles, thus the angular dependence of vegetation indices is of particular concern in remote sensing product validation. The 4-Scale model (Chen and Leblanc, 1997), based on detailed consideration of canopy architecture, is used to investigate the implications of the bidirectional reflectance distribution function (BRDF) on vegetation indices for four boreal forest canopies (old black spruce, young and old jack pine, and old aspen). The model is used to systematically simulate the effects on the Normalised Difference Vegetation Index (NDVI) of different viewing and illumination geometries and canopy architecture (tree crown volume, reflectivity of the soil and foliage, non-random distribution of the trees, tree density and LAI). The model reproduces closely the angular distributions of NDVI measured in the four stands. It is shown that the directionality of NDVI depends on many canopy architectural parameters and the differences in the foliage and background optical properties, indicating considerable uncertainties in deriving biophysical parameters from two-band vegetation indices when the directionality information is not used and canopy architectural parameters are unknown.

1. Introduction

Validation of satellite-derived high-level products, such as biophysical parameter fields, requires correction of intermediate variables used in the derivation of the products. The variables include spectral reflectances at the surface level and vegetation indices formulated from the reflectances. Two-band vegetation indices (VI) based on the reflectance in the red and near-infrared (NIR) bands, measurable remotely are used as quantitative measures of vegetation on the Earth's surface. One of the most commonly used VIs is the Normalised Difference Vegetation Index (NDVI) calculated as (Rouse et al. 1974):

$$NDVI = \frac{\rho_{NIR} - \rho_{RED}}{\rho_{NIR} + \rho_{RED}} \tag{1}$$

where ρ_{NIR} and ρ_{RED} are the reflectances in the NIR and red bands, respectively. Although the NDVI has been criticised for its inability to discriminate the effects of different soil background (Huete, 1988), it has been found to remove some of the noise in remote sensing signals through taking the ratio between the two bands (Chen, 1996a; Peterson et al., 1987). This is particularly important in boreal forest environment where small contrasts often exist between the optical properties of the forest foliage and the background (soil and understorey). In this paper, we focus on the NDVI only. Other indices such as the Simple Ratio (SR) and Modified Simple Ratio (MSR) (Chen, 1996a) can be calculated from NDVI.

It is well known that the reflectance in optical bands from forest stands depends strongly on illumination and view angles (see Myneni and Ross, 1991). The main feature in the bidirectional reflectance distribution of forest canopies is the hotspot which occurs mainly because of the shadow-hiding process (Hapke et al., 1996). Although the angular distribution patterns are often similar in both red and NIR bands for a large range of views (Bréon et al., 1996; Leblanc et al., 1999), vegetation indices based on the ratio of these two bands, such as NDVI, still contain significant angular variation because of the subtle differences between the bands (Gutman, 1991). Airborne reflectance measurements taken with the POLDER (POLarization and Directional Earth Radiation) instruments (Deschamps et al., 1994; Bréon et al., 1996) at an altitude of about five kilometres (see Fig. 1) and ground-based PARABOLA (Portable Apparatus for Rapid Acquisition of Bidirectional Observations of Land and Atmosphere) measurements (Deering et al., 1994 and 1995) indicate a directional dependence of NDVI on the view zenith angle (VZA). Measurements of tallgrass prairie (Middleton, 1991) and alfalfa (Pinter, 1993) also show a dependence of NDVI on the solar zenith angle (SZA). Relationships between two-band VIs and leaf area index (LAI) of conifer forests in the United States were found by Peterson et al. (1987) using the Airborne Thematic Mapper and Spanner et al. (1990) using the Advanced Very High Resolution Radiometer. Landsat TM images were successfully used by Fassnacht et al. (1997) to relate individual bands and several vegetation indices to the LAI of 24 deciduous, conifer and mixed stands. Chen and Cihlar (1996) reported significant correlations between NDVI obtained from Landsat TM images and LAI in boreal conifer stands. These successful studies with Landsat images acquired within small view and solar zenith angle ranges indicate the usefulness of vegetation indices for LAI mapping when their angular variability is removed and cover type information is used.

Since measurements are available for a limited number of sites and conditions, radiative transfer models are often used to assess the influence of canopy attributes on the NDVI (Goel and Qin, 1994; Goward and Huemmrich, 1992; Huemmrich and Goward, 1997; Moreau and Li, 1996;n Myneni and Williams, 1994, Rosema et al., 1992). The NDVI directionality, although implicitly included in previous BRDF studies (e.g., Li and Strahler, 1992; Nilson and Peterson, 1991; Verhoef, 1984), has not been comprehensively investigated for forest stands. The 4-Scale model recently developed by Chen and Leblanc (1997) provides a useful tool for studying the influence of canopy architecture on the NDVI. The 4-Scale model is based on a detailed mathematical description of canopy architecture at the scales of tree group, tree crown, branch, and shoot or leaf (see the next section for details). Using remotely sensed measurements and the 4-Scale model, the objectives of this paper are: (1) to show the causes of NDVI directionality in forest canopies, and (2) to show the implications of its directionality in the derivation and validation of biophysical parameter maps of boreal forests.

2. Four-Scale model

The 4-Scale radiative-transfer model (Chen and Leblanc, 1997; Leblanc et al., 1999) was developed with emphasis on the structural composition of forest canopies at different scales. The 4-Scale is a geometric-optical model employing several new modelling methodologies:

(1) The non-random spatial distribution of trees is simulated using the Neyman type A distribution (Neyman, 1939) that creates patchiness of a forest stand. The model simulates tree

crowns as discrete geometrical objects: cone and cylinder for conifers, and spheroid for deciduous species. The size of the crowns decreases when the trees are found in large clusters and the tree locations are also subject to the repulsion effect (i.e., no vertical overlaps occur) to better represent the competition for light;

(2) Inside the crowns, a branch architecture defined by a single inclination angle (Chen and Black, 1991) is included to improve the calculation of light penetration from the geometric-optical model of Li and Strahler (1992) which used the assumption of random leaf distribution inside tree crowns. A branch is in turn composed of foliage elements (individual leaves in deciduous and shoots in conifer canopies) with a given angle distribution pattern;

(3) The hotspot is computed both on the ground and on the foliage with gap size distributions between and inside the crowns, respectively;

(4) The imaginary tree surface created by the crown volume (cone and cylinder, or spheroid) is treated as a complex medium rather than a smooth surface so that shadowed foliage can be observed on the sunlit side.

For optimum results, the model has multiple parameters that can be separated into three categories: (i) site parameters: domain size (which represents the pixel size), leaf area index (LAI), tree density, tree grouping factor (m_2) in the sub-domain size (quadrat), solar and view geometry (SZA, VZA and azimuthal angle difference ϕ); (ii) tree architecture parameters: crown radius (r), crown height (H_b) and height base (H_a), apex angle (α) and needle-to-shoot area ratio (γ_E) for conifers, foliage distribution ($G(\theta)$, the projection of unit leaf area with the clumping index g or the branch architecture with leaf or shoot orientation α_L, branch inclination α_b, foliage thickness R_L, branch leaf area index L_L and branch thickness R_b), clumping-index (Ω_E) and typical size of the foliage elements (W_s); and (iii) optical properties (reflectivities) of the foliage and the ground at desired wavelengths. When measurements are not available for some parameters, defaults or best estimates can be used. The reflectance is calculated by associating the reflectivities of the crown (R_T and R_{ZT} for sunlit and shaded crown, respectively) and the background (R_G and R_{ZG} for sunlit and shaded background, respectively) to the four scene components (proportions of the domain viewed): sunlit (P_T) and shaded crown (Z_T) and sunlit (P_G) and shaded background (Z_G):

$$\rho = P_T \cdot R_T + P_G \cdot R_G + Z_T \cdot R_{ZT} + Z_G \cdot R_{ZG} \tag{2}$$

A distinction is made here between reflectivity and reflectance. While both refer to the percentage of incident radiation reflected by an object, "reflectivity" is used for scene components such as sunlit foliage and ground, however "reflectance" is used for the composite scene, i.e., the overall scene reflectance. This distinction bridges the gap in terminology usage between ecologists and remote sensing scientists. For the shaded components, the reflectivity is defined as the percentage of reflected irradiance from those components per incident solar irradiance at the top of the canopy for the convenience of modelling. The sunlit components are mainly governed by the direct irradiance and their intrinsic reflectivities while the reflection from the shaded components depends on their irradiance resulting from the sky diffuse radiation and multiple scattering within the canopy. Average multiple scattering factors (Chen and Leblanc,

1997) are used over the whole SZA range. The contribution of multiple scattering is more important in the NIR than the red band because of the larger foliage reflectivity and transmisivity. For a canopy with an important understorey such as hazelnut shrubs in the BOREAS Old Aspen site, a double-canopy version of the 4-Scale model is used (Leblanc et al., 1999). The double-canopy introduces two new proportions in equation (2), namely shaded and sunlit foliage in the lower canopy. The model results compare very well with airborne POLDER data (Leblanc et al., 1997) of four boreal forests (coefficients of determination (R2) larger than 0.90) and ground PARABOLA measurements (Chen and Leblanc, 1997) taken over the Old Black Spruce (OBS) stand used in BOREAS (BOReal Ecosystem-Atmosphere Study, Sellers et al., 1991). Table 1 shows the model input parameters, based on measurements in the BOREAS sites (Chen 1996a and 1996b; Chen and Cihlar, 1996; Chen et al., 1997; Middleton et al., 1997; White et al., 1995). Variations of these parameters are applied here to study different optical, architectural, and directional effects on the NDVI.

	OBS	YJP	OJP	OA aspen/hazelnut (single)
Latitude N	53.985°	53.975°	53.916°	53.629°
Longitude W	-105.12°	-104.65 °	-104.69°	-106.20°
Domain size	1 ha	1 ha	1 ha	1 ha
θ_s	33.5°	37.2°	35.0°	39.3°
LAI	4.5	2.7	2.2	1.5 / 0.5 (1.5)
Tree Density	4000 trees/ha	4000 trees/ha	1850 trees/ha	850 / 6000 trees (850) /ha
Tree grouping (m_2)	4	3	3	3 / 0
Quadrat size	500 m^2	500 m^2	500 m^2	285.7 m^2
H_a	0.5 m	0.5 m	7.0 m	11.0 / 0.0 (11.0) m
H_b	6.5 m	2.5 m	4.0 m	7.0 / 2.0 (7.0) m
$H_o(\alpha, r)$	1.9 m	1.5 m	3.2 m	–
r	0.45 m	0.85 m	1.30 m	1.90 / 1.00 (1.9) m
α	13°	30°	22°	–
α_b	–	15°	15°	–
α_L	–	80°	80°	–
L_L	–	0.8	0.8	–
$G(\theta)$	0.5	–	–	0.5 / 0.5 (0.5)
W_a	0.035 m	0.17 m	0.05 m	0.10 / 0.02 m (0.10)
γ_E	1.41	1.43	1.30	–
Ω_E	0.70	–	–	0.80/0.98 (0.8)
R_L	–	0.2	0.2	–
R_b	–	0.1 m	0.1 m	–
R_T (red)	0.11	0.05	0.07	0.07 / 0.06 (0.07)
R_{ZT}(red)	0.003	0.005	0.003	0.01 / 0.02 (0.01)
R_T (nir)	0.50	0.53	0.53	0.50 / 0.50 (0.5)
R_{ZT}(nir)	0.11	0.19	0.13	0.20 / 0.30 (0.20)
R_G (red)	0.04	0.05	0.09	0.04 (0.05)
R_{ZG}(red)	0.002	0.004	0.003	0.02 (0.01)
R_G (nir)	0.25	0.15	0.17	0.20 (0.25)
R_{ZG}(nir)	0.11	0.08	0.09	0.15 (0.2)

Table 1: Model input parameters for the four canopies taken from Leblanc et al.(1999). The parameters for the OBS, YJP, and OJP sites are based on summer conditions and the parameters for the OA site represent Spring conditions.

3. Directionality of NDVI in forest stands

Figure 1 shows POLDER measurements and the 4-Scale simulated NDVI near the principal solar plane (azimuth angle within 10°) for four boreal forest sites (the red and NIR measurements and simulations can be seen in Leblanc et al., 1999). The input parameters for the model are listed in Table 1 with the red band centred at 670 nm and the NIR band at 864 nm. Only the OBS site shows important differences between the simulation and the measurements at small VZA that mainly come from the differences between the measured and modelled red band reflectance. The discrepancies at large VZA on the forward scattering side of OBS and OA could be caused by the atmospheric correction algorithm used (Leblanc et al., 1999).

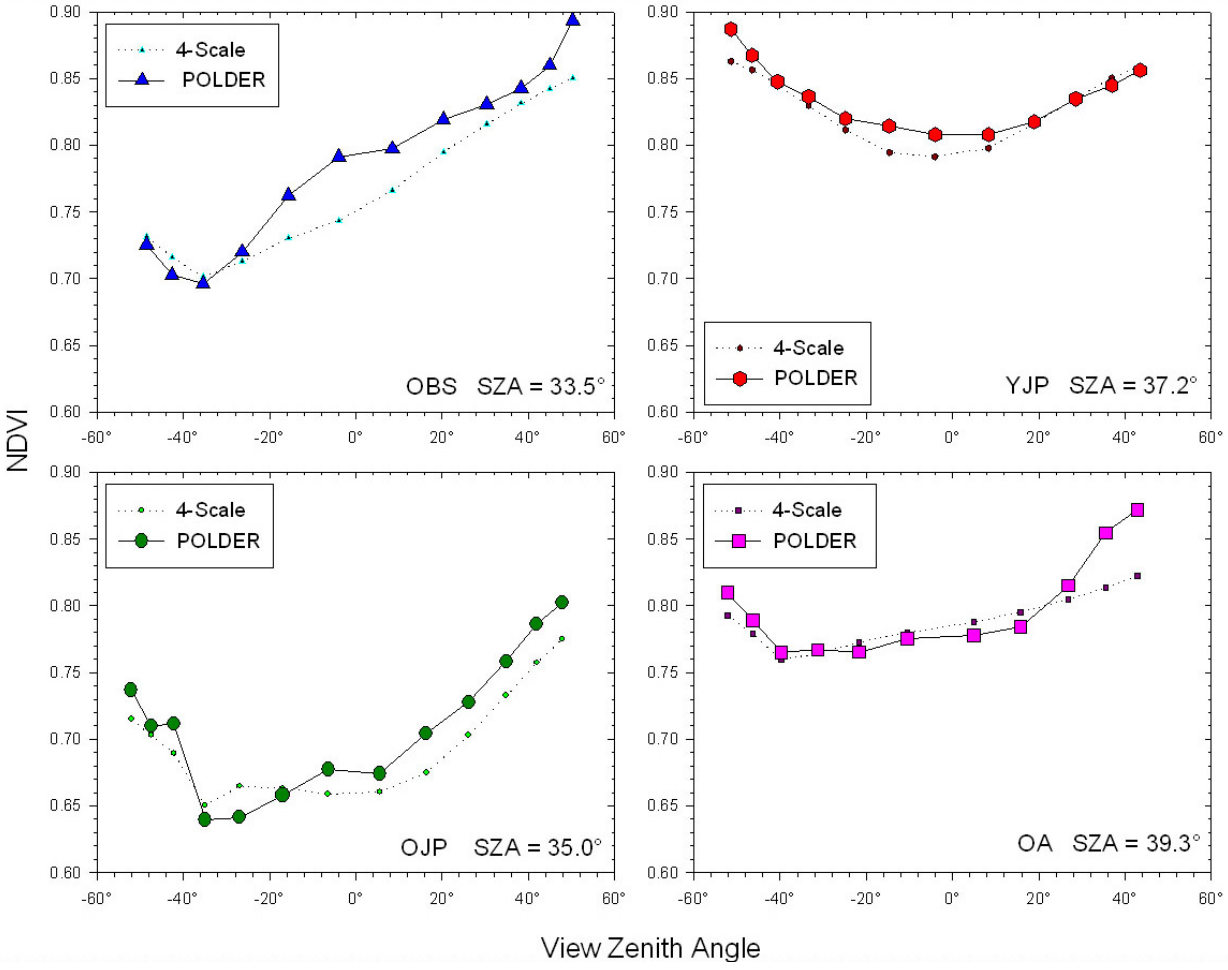

Figure 1: Surface NDVI calculated from the red and near-infrared band of the POLDER instrument with the atmospheric correction algorithm 6S (Vermote et al, 1996), and NDVI simulated with the 4-Scale model for four boreal forest sites: Old Black Spruce (OBS), Young Jack Pine (YJP), Old Jack Pine (OJP) and Old Aspen (OA). The parameters in Table 1 are used as inputs for the model.

Figures 2a and 2b show the directional reflectance distributions of the OBS stand in the red and NIR bands, respectively. The results are obtained using the 4-Scale model with the parameters from Table 1 but at SZA=45°. The simulations show strong directional dependency and

pronounced hotspots in both bands. In open boreal forests, the influence of the background on the directional distribution is particularly strong. Because NDVI is computed using reflectances in the red and NIR bands, it is also influenced by the view and illumination geometry, even though a large portion of the angular variability is reduced after taking the ratio of these two bands.

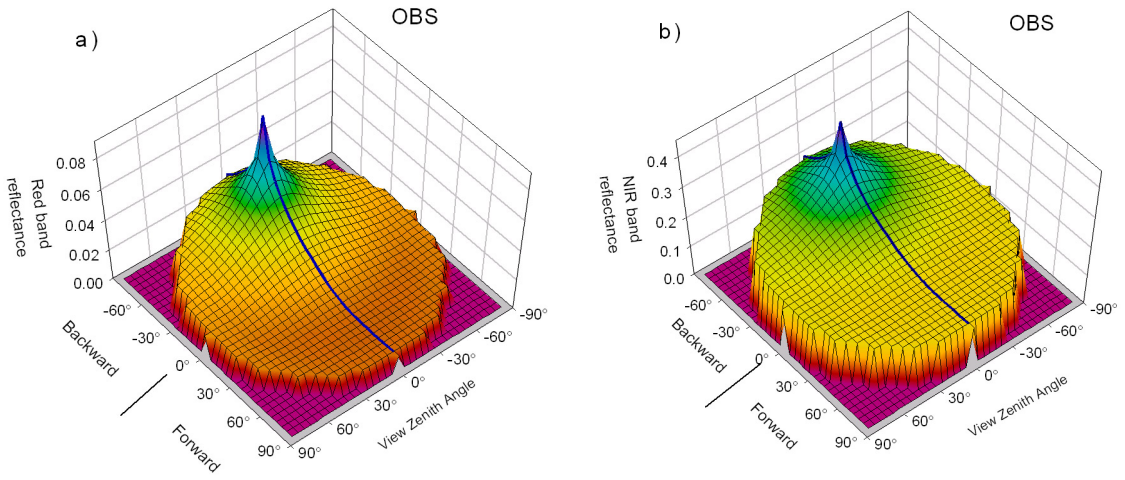

Figure 2: Hemispherical reflectance simulations of the Old Black Spruce site in a) the red band abd b) the near-infrared band. The blue grid line represents the principal solar plane. SZA = 45°.

Figure 3a shows a hemispherical distribution of the NDVI using the data shown in Figs. 2a and 2b for the OBS site. The NDVI is largest on the forward scattering side with values up to 0.85 and lowest at the hotspot with a value of 0.65. At the hotspot, the scene is composed of only sunlit crown and ground, both of which have lower NDVI than their shaded counterparts. Sunlit components are dominated by the direct irradiance while the shaded components reflect diffuse radiation from the sky and from multiple scattering. In the NIR band, which is more affected by the multiple scattering than the red band, the relative increase of shaded components brightness from multiple scattering is larger than that in the red band, giving rise to a larger NDVI in the shaded components than in the sunlit components. Figure 3b shows a simulated hemispherical distribution of NDVI for the BOREAS YJP site. The range of NDVI distribution at YJP is narrower than at OBS. It increases from 0.78 at the hotspot to a maximum of 0.91 at large view zenith angles. Although the range of directional variation in NDVI is substantially smaller than those of the individual bands, it is still considerable in both cases.

Figure 4 shows simulated NDVI distributions along the principal planes for the four sites investigated at a common SZA of 45°. The simulations were done at a view angle step of one degree. The measured and simulated NDVI from Fig. 1 missed the hotspot effect because of the large angular separation (5° to 12°) used. Generally, the NDVI increases as the view zenith angle increases, and is larger on the forward scattering side than on the backward scattering side. The NDVI distributions on both sides are more symmetrical in YJP and OA than in OBS and OJP. The model is now used to reveal the reasons behind these different NDVI angular distributions at the various sites and to investigate in general the effects of ground and foliage optical properties and various canopy architectural attributes on NDVI distribution.

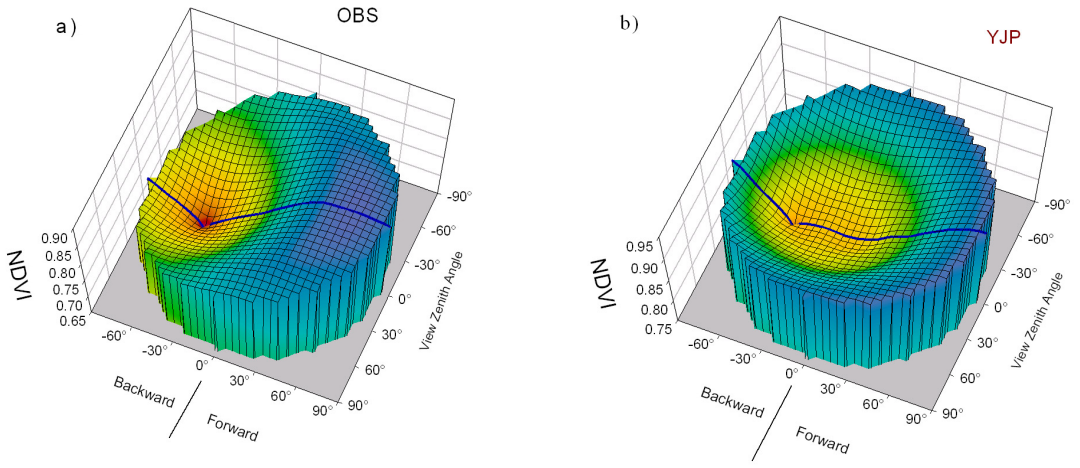

Figure 3: Hemispherical NDVI simulations of a) the Old Black Spruce site and b) the young Jack Pine site. The thicker grid line represents the principal solar plane. SZA = 45°.

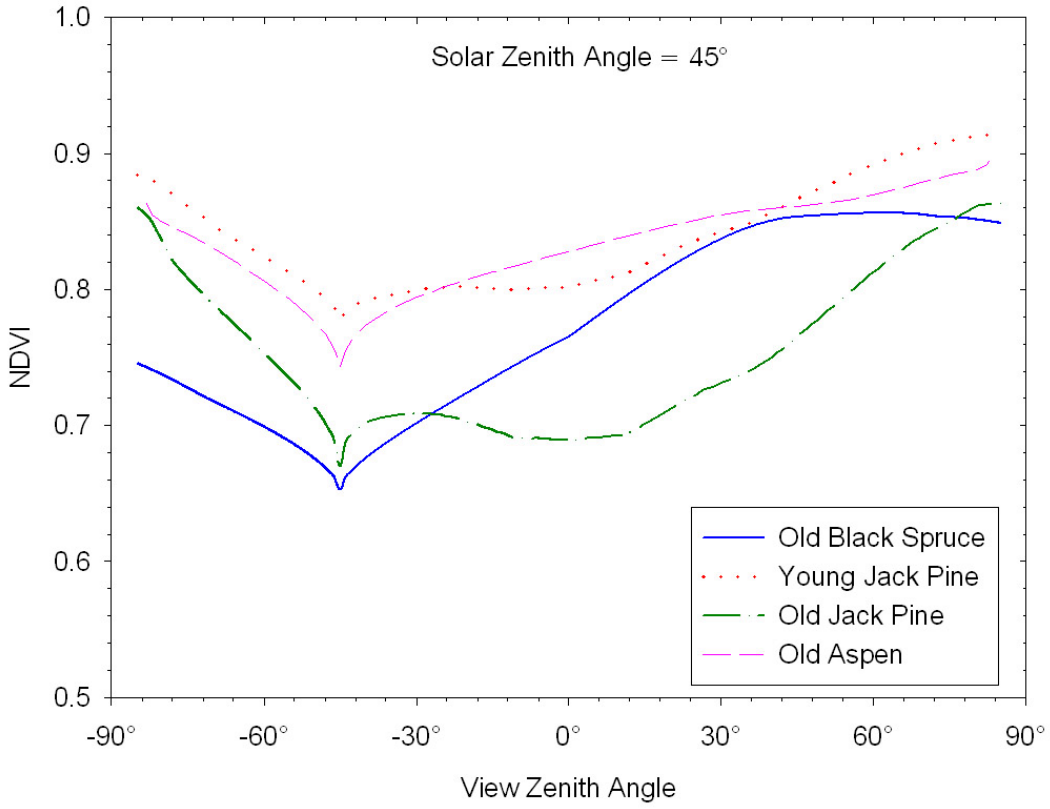

Figure 4: Simulated NDVI in the principal plane for four boreal forests: Old Black Spruce, Young Jack Pine, Old Jack Pine, and Old Aspen. SZA = 45°.

3.1. The effects of the solar zenith angle

The sun's angular position has a great influence on remote sensing signals from forest canopies, especially near the hotspot and nadir views. The latter is extremely important because of the effect of SZA on the amount of shaded ground surface that can be seen from remote sensing platforms. Measurements in tallgrass prairie (Middleton, 1991) and in alfalfa (Pinter, 1993) generally show an increase of NDVI with SZA. However, Singh (1988), and more recently Sellers et al. (1995) using a simple angular correction algorithm (FASIR), assumed a decrease of NDVI with increasing SZA. The knowledge for this specific SZA effect is lacking for the boreal forest. Figure 5 shows nadir NDVI changes with SZA. The four simulated canopies all show an increase of NDVI with SZA, due to a common reason: with an increasing SZA, more shadowed foliage and background is seen vertically, and the shadowed components have higher NDVI than their respective sunlit counterparts. The simple treatment of the complicated multiple scattering effect may have induced an unknown error in calculated NDVI distribution when SZA is larger than 60° .

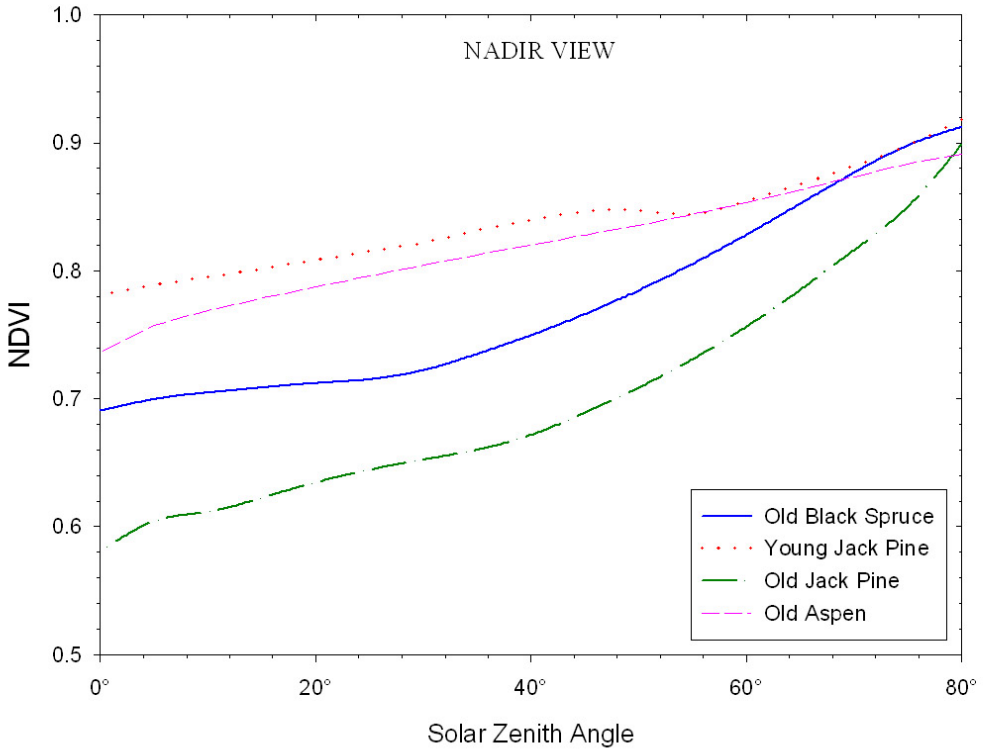

Figure 5: NDVI versus solar zenith angle for four boreal forests simulated using the 4-Scale model.

3.2. The effects of ground and foliage reflectivities

The proportions and reflectivity combinations of the four scene components are the main mechanisms behind the directionality of NDVI in forest stands. The background usually has a lower NDVI than the foliage so that an increase in LAI, which reduces the gap fraction, results in a larger NDVI. This is the main reason for the general bowl shape of NDVI hemispherical

distribution shown in Fig. 3. The increase in the probability of seeing shaded foliage at large view zenith angles also contribute to the bowl shape. For two forests with similar probabilities of seeing sunlit and shaded components but with different scene reflectivities, their NDVI values can be very different. The reflectivities of each scene also depend on the sensors band and bandwidth used (Teillet et al., 1997).

Figure 6a shows simulated NDVI distributions in the principal solar plane at SZA = 45° for the OBS site for four cases of background reflectivities: (1) normal case with the background reflectivities based on measurements; (2) normal NIR background reflectivities but with double red band reflectivities (R_G^{RED} = 0.08 and R_{ZG}^{RED} = 0.004); (3) normal red band reflectivities with double NIR band reflectivities (R_G^{NIR} = 0.50 and R_{ZG}^{NIR} = 0.22); and (4) a very reflective background with double red and NIR reflectivities (R_G^{RED} = 0.50, R_{ZG}^{RED} = 0.08, R_G^{NIR} = 0.22 and R_{ZG}^{NIR} = 0.004). The results indicate that the changes are more important at nadir where the maximum background can be seen. The two extreme cases are found when only one of the bands is changed. Doubling the NIR band background reflectivities increases the nadir NDVI, and doubling the red decreases it by the same amount. When both band's background reflectivities are increased, the NDVI is much less affected because the ratio of the bands remove some of the variations. Figure 6b shows, as examples, how NDVI is affected by a variation in the red foliage band reflectivities. Low (R_T^{RED} = 0.073 and R_{ZT}^{RED} = 0.003) and high (R_T^{RED} = 0.165 and R_{ZT}^{RED} = 0.006) foliage reflectivities are used to demonstrate the effect of foliage reflectivity on NDVI. The lower red reflectivity induces a larger NDVI and the higher reflectivity gives the opposite.

3.3. The effects of leaf (shoot) and branch inclinations.

Branch and leaf (or shoot for conifers) inclinations also affect the directionality of the NDVI. The processes of both light and view line penetrations through the canopy are influenced by the orientation of the foliage. The 4-Scale model simulates the sub-canopy architecture with branches symmetrically attached around the trunk. The leaves or shoots are found within the branches defined as thin slabs of foliage. The branch and leaf inclinations (α_b and α_L) from the horizontal plane are the parameters that control the sub-canopy architecture (Chen and Black, 1991). Detailed 3-D measurements of the architecture of jack pine trees can be found in Landry et al. (1997).

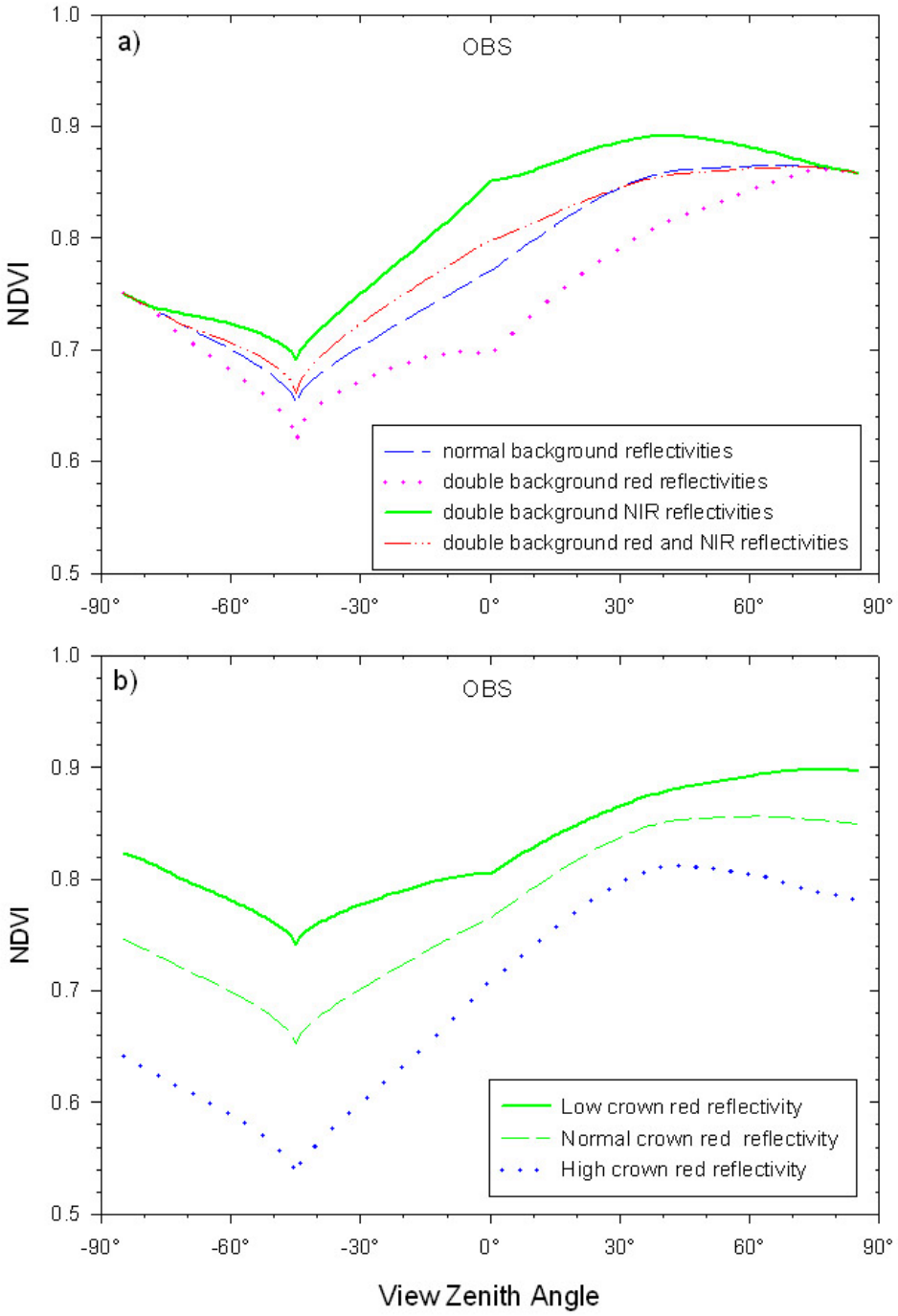

Figure 6: Effects of a) the variation of the ground reflectivity and b) the variation of the foliage reflectivity in the red band on the principal plane NDVI of the Old Black Spruce site. SZA = 45°.

Figures 7a and 7b show the difference in NDVI between the cases of near vertical (α_b = 75° and α_L = 75°, positive angles representing upward directions) and horizontal branches and shoots (α_b = 0° and α_L = 0°) for the OBS and OJP site, respectively, at SZA = 45°. The branches and shoots are randomly distributed within their respective confinement: shoots within branches and branches within tree crowns (Leblanc et al., 1999). The branch architecture has a pronounced

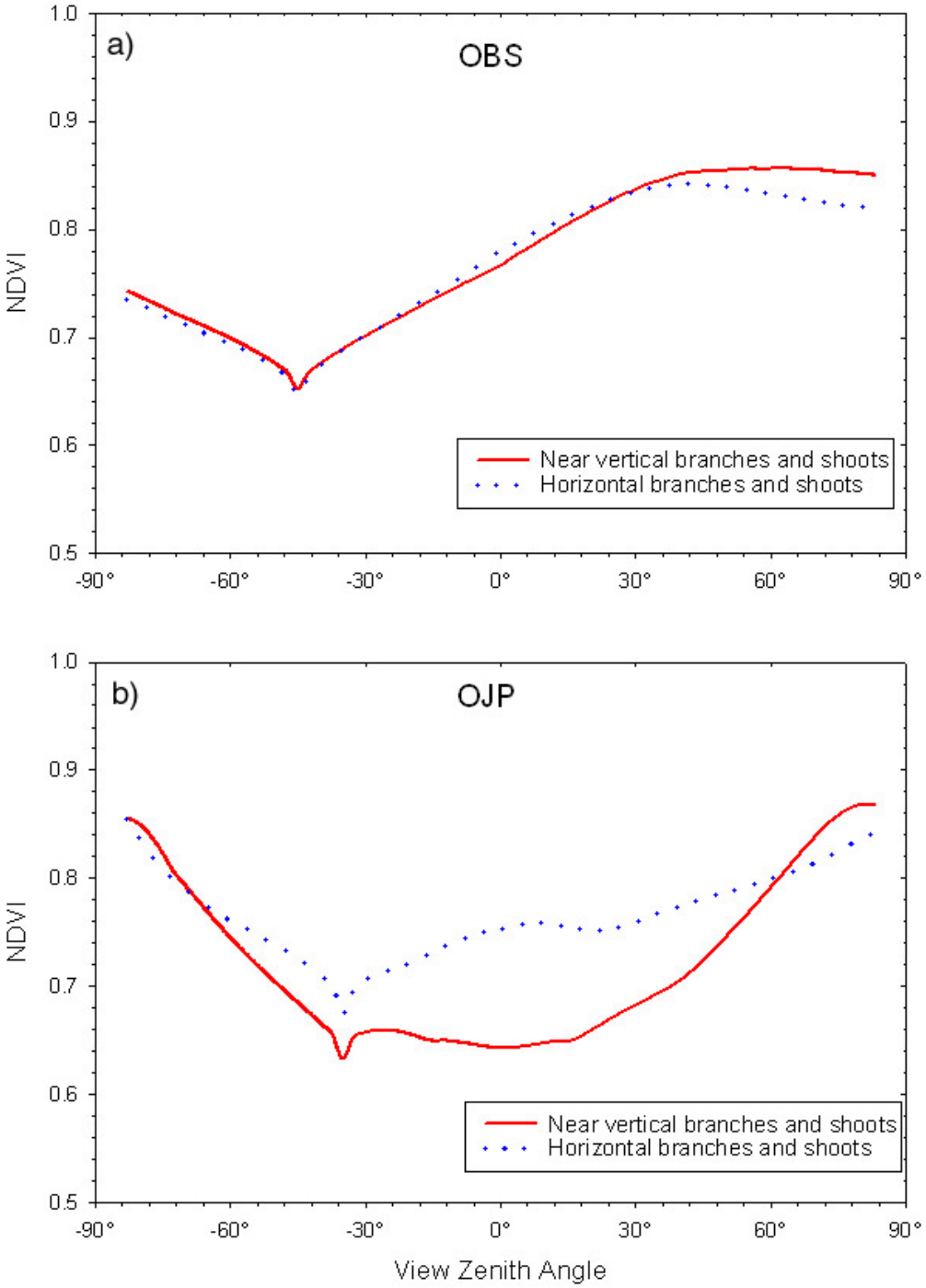

Figure 7: The principal plane NDVI with horizontal and near vertical shoots and branches for a) the OBS site and b) the OJP site. SZA =°.

effect on the directional distribution of NDVI in OJP, but the effect is much smaller in OBS. The difference in crown foliage density in these two stands is the probable cause for the difference in the magnitude of the sub-canopy architecture effect. The foliage density in OJP crowns is low and therefore the change in the foliage organization and orientation has a large effect on the probabilities of light and view line penetrations through the crowns. In OBS, where tree crowns

are dense, the model shows that detailed foliage distribution within the crowns only has a secondary effect on NDVI. In both cases, similar patterns of sub-canopy architectural effects are found, albeit different in magnitude. Near nadir, the NDVI is larger in the case of horizontal shoots and branches because the probability of seeing the background vertically is smaller through the horizontal foliage. At large view zenith angles on the forward scattering side, the foliage orientation increases the NDVI. When the branches and shoots are horizontal, the probability of seeing sunlit foliage from the shaded side is larger than when the foliage is almost vertical. The dense vertical structure prevents the viewer to see sunlit foliage through the crown. Again, the NDVI increases because the viewer sees more shaded foliage. This sub-canopy architectural effect should depend on the stand density, which modifies the multiple scattering processes. The 4-Scale model needs to be improved for investigation of the multiple scattering effects for a larger range of stand densities. The multiple scattering should be explicitly included and the code improved because it is limited numerically to a maximum probability of about 350 trees per sub-domain in the combined Neyman and negative binomial functions.

3.4. The effects of crown volume

The crown volume confines the spatial distribution of the foliage. Using the 4-Scale model, variations of the crown's radius (r) and height (H_b) are applied to the OBS and OJP sites. One effect of using larger radius is to decrease the gap fraction, especially near the vertical direction. A smaller gap fraction means less background to be seen and therefore a larger NDVI. Figure 8a shows NDVI distributions on the principal plane for the OBS site, the curves representing different crown volumes using a constant LAI. At very large view angles on the forward scattering side, the NDVI increases as the crown radius decreases because the foliage density inside the crowns increases, thus allowing less sunlit foliage to be seen on shaded side of the crown. By changing the length of the cylinders, the model shows NDVI variation mainly on the forward scattering side where taller crowns cast longer shadows. Although the foliage density inside the crown decreases with crown height, the amount of shaded foliage seen at large zenith angles increases on the forward scattering side, resulting in a NDVI increase. Comparing Figs. 8a and 8b shows that the crown volume does not change the NDVI at OJP the same way as at OBS. Because the LAI is lower and the gap fraction larger at OJP than at OBS, changing the crown volume induces more pronounced effects on the NDVI in OJP. The major NDVI changes of OJP can be seen at nadir on Figure 8b.

3.5. The effects of stand density and LAI

Theoretically, a forest vegetation index indicates the amount of foliage in a forest, thus it should be related to the LAI. In open boreal forests, NDVI-LAI relationships can be greatly affected by the contribution from the background consisting of various understory species and mosses. The amount of the background contribution is highly dependent on the stand density. 3.5. The effects of stand density and LAI Theoretically, a forest vegetation index indicates the amount of foliage in a forest, thus it should be related to the LAI. In open boreal forests, NDVI-LAI relationships can be greatly affected by the contribution from the background consisting of various understorey species and mosses. The amount of the background contribution is highly dependent on the stand density.

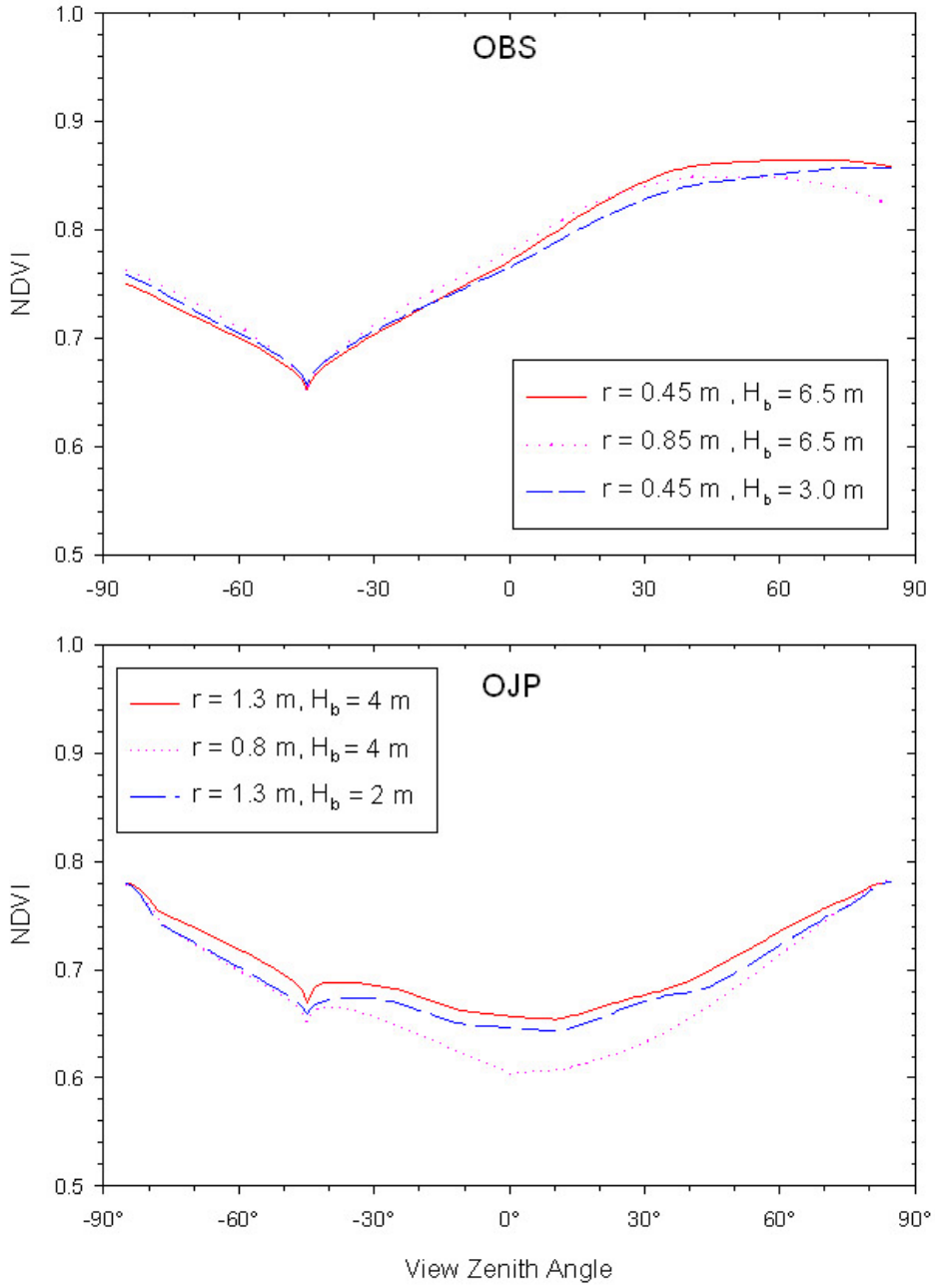

Figure 8: Effect of crown volume on the directionality of NDVI; variation of the crown radius and height for a) the OBS site and b) the OJP site. SZA = 45°.

Figure 9 shows the variation of NDVI at the OA site in the principal plane with different LAI values and tree densities. The results indicate that a LAI of 1.5 can give a larger NDVI than a LAI of 3 for the same species if the foliage is distributed in more tree crowns of the same size. For the same number of trees, a higher LAI produces a larger NDVI. A change in the understorey LAI is also simulated with the LAI of the hazelnut at 0.5 and 2 for the aspen canopy with LAI of 3. It shows that the LAI of the hazelnut is an important factor as it increases the NDVI. The complications induced from the variations in the stand density, crown size and background may be the reason for weak NDVI-LAI relationships found in previous studies (Badhwar et al., 1986).

In reality, dense stands do not show much deviation from a random tree distribution (Franklin et al., 1985), so when averaged for large areas, it causes only a small uncertainty in NDVI-LAI relationships for coarse resolution images. However, in high resolution images, the dependence of the NDVI on the stand density can be a large source of error in LAI mapping because of large variations in stand density due to patchiness caused by many local variations in environmental conditions.

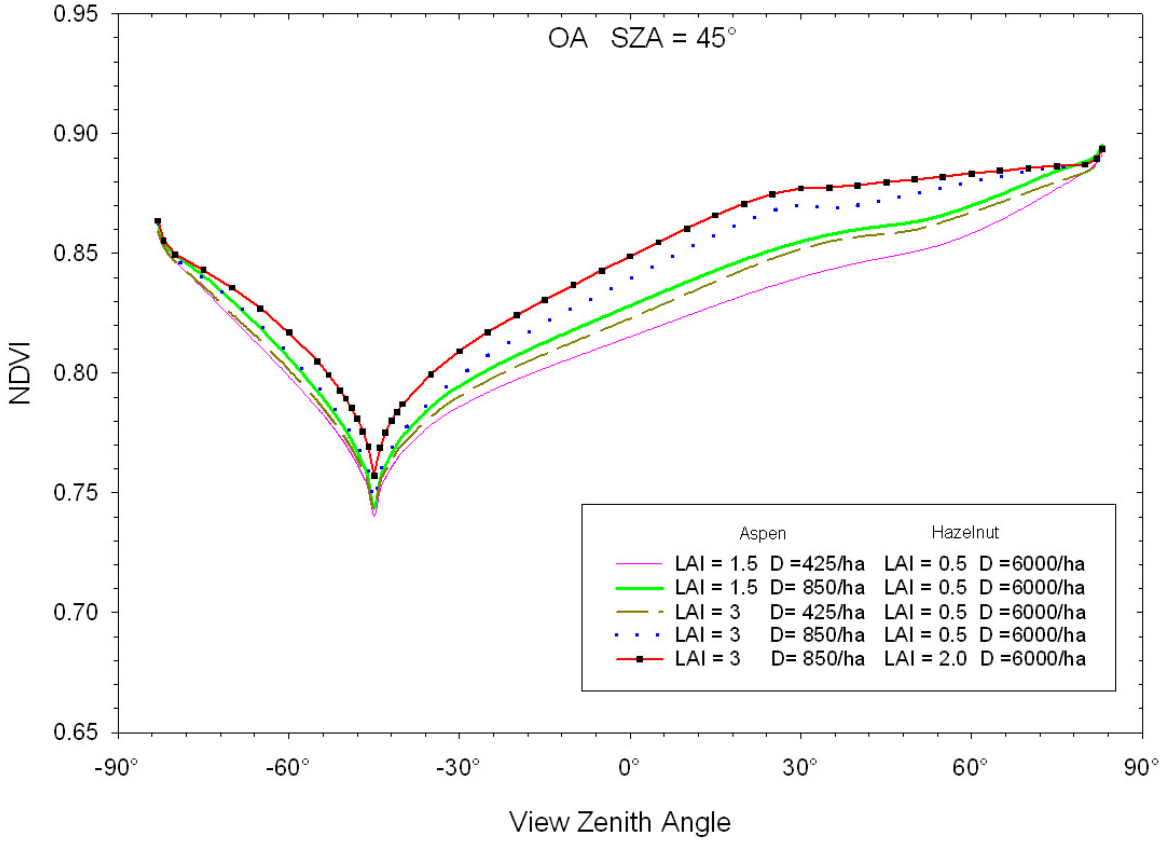

Figure 9: Effects of LAI and stand density on NDVI of the OA site. SZA = 45°.

3.6. The effects of tree distribution patterns

The patchiness of a forest stand, or the non-randomness of tree distribution, is modelled using the Neyman distribution in the 4-Scale model. The domain is divided into n quadrats. The size of the quadrats represents the extent of the radiative interaction process within the canopy, i.e., the horizontal distance of light (or view line) penetration from the top of the canopy to the ground. It should also be adjusted for the maximum extent of a cluster of trees. The non-random tree distribution is obtained by having random positioning of clusters of trees with a random size, i.e., a double Poisson process. The mean cluster size is the Neyman grouping m2. In our previous studies (Chen and Leblanc, 1997; Leblanc et al., 1999), we used large quadrat sizes to consider the interaction at large zenith angles but at small zenith angles, or when the foliage density is high, the interaction occurs only within a small spatial distance and the grouping of trees within the quadrat thus becomes very important. When using a quadrat size of 500 m2, the Neyman grouping has a small effect on the reflectances (Chen and Leblanc, 1997), but by reducing the

quadrat size to 100 m^2, the Neyman process greatly affects the reflectances, and thus the NDVI. Measurements in the OJP site revealed a m_2 value of 3 for quadrat size of 100 m^2 (Chen and Leblanc, 1997). Increasing the grouping factor m2 augments the stand patchiness and the probability of seeing the ground. Figure 10 shows how the NDVI changes with different Neyman groupings. The random case is modelled with the Poisson distribution. The variation around nadir is mainly due to the effect of tree grouping on light penetration in the canopy. The tree grouping only has a small effect on the gap fraction near the vertical view direction when the repulsion effect is used (i.e., when no vertical overlapping of the crowns is allowed). The grouping effect allows more sunlight to reach the ground surface, giving less shaded ground surface, thus smaller NDVI values.

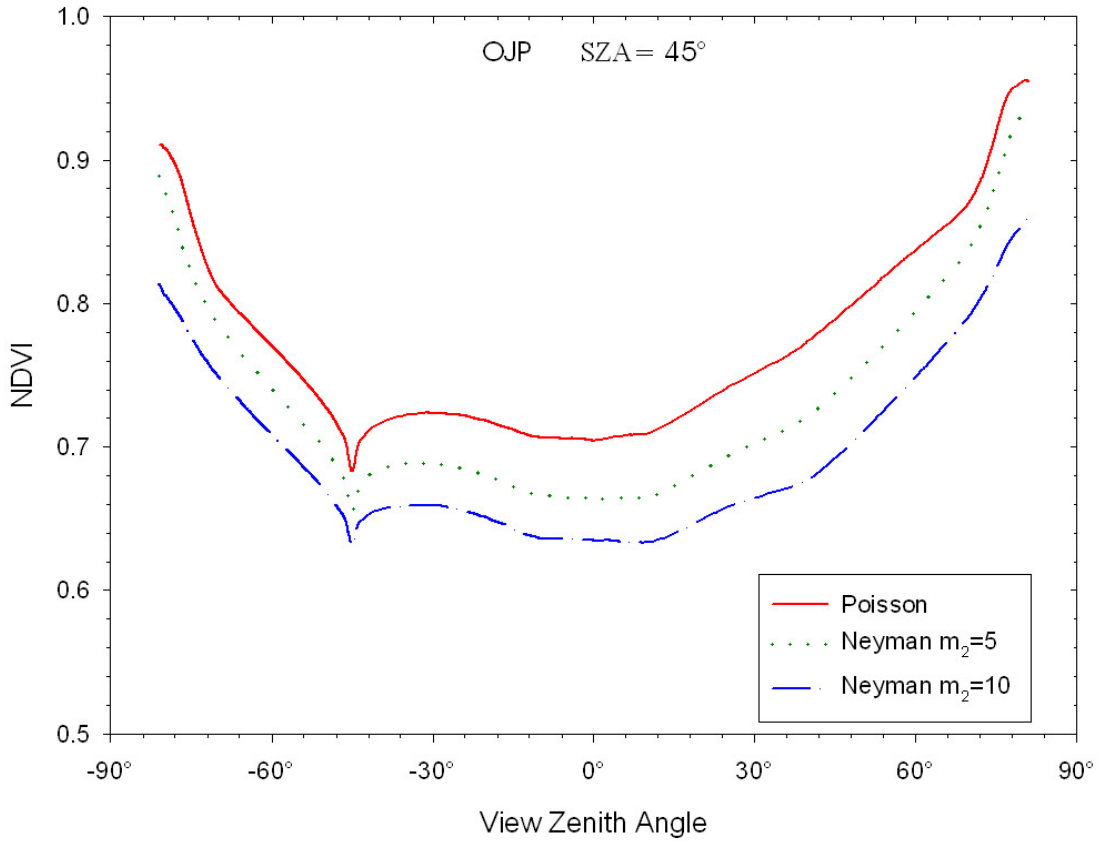

Figure 10: Tree clustering effects on NDVI in the OJP site. SZA = 45°. The Neyman grouping m_2 is the mean cluster size.

3.7. Main mechanisms controlling the NDVI for the four sites

With the simulation results shown in Figs. 6-10, we can now explain the mechanisms controlling the measured NDVI distributions in Fig. 1. The four scene components that compose the reflectances have different NDVI values that are determined by their red and NIR reflectivities. For all four sites, the largest scene component NDVI values are associated with the shaded components, and they are generally higher for the canopy than the background. Since the probabilities of seeing both shaded and sunlit crowns increase with view zenith angle, the NDVI

values follow the same trend which results in a directional distribution of NDVI that is minimum at the hotspot where all the foliage and the ground scene components are illuminated, or at nadir where the maximum background can be seen, depending on the reflectivities and the scene proportions. NDVI variations near the hotspot can be seen more clearly in the simulations shown in Fig. 4 than those in Fig. 1 where the POLDER measurements were only available in large angular steps. It was shown that any changes in the gap fraction due to crown size, view angle, foliage density, etc., affects the NDVI, as more ground seen through the canopy generally decrease the NDVI.

Based on the reflectivities in Table. 1, the NDVI value for the shaded ground component in the OBS site is the largest among the four sites investigated because of the green moss and understory species. The OBS NDVI increases continuously from the hotspot to the nadir and to the large view zenith angles on the forward scattering side. This is mainly caused by the continuous increase in the probabilities of seeing the shaded crown. The elongated crowns at the OBS site cause the canopy gap fraction to decrease rapidly from the nadir. This is one explanation of the steeper change in the NDVI value with the VZA than the other sites where crowns are larger and the gap fraction varies less with the VZA. In OBS, the lowest NDVI at large backscattering VZAs is associated with the lowest NDVI for the sunlit crown (0.65) among the four species. On the forward scattering side at VZAs larger than 55°, the modelled NDVI in OBS (Fig. 4) shows a decreasing trend because of the cone and cylinder geometry. At large zenith angles, the cylindrical part of the crown is obscured and the scene is occupied mostly by the conical part. Because of the conical geometry, a small sunlit surface can be seen from the shaded side combined with a high red foliage reflectivity causes a decrease in the NDVI value. However, this trend is not found in the measurements because of the limited view angle range. The OBS site has the largest LAI (Table 1) but because the foliage is concentrated in dense pencil-like narrow crowns, the resulting NDVI is not the largest.

The low NDVI in OJP is caused by a combination of three factors: (i) a low tree density (1850 stems per hectare); (ii) a small LAI (2.2); and (iii) the lowest sunlit ground NDVI among the species studied. Both (i) and (ii) result in large canopy gap fractions. Near the vertical view direction, about half of the exposed ground in OJP is illuminated at SZA = 35°, resulting in the lowest NDVI among the four forest stands.

The YJP and OA sites have the highest NDVI among the four sites studied within the principal solar plane. The large NDVI in YJP can be explained by the reflectivities of the scene components (see Table 1). The YJP site has a low LAI but with a larger crown size, hence the gap fraction is smaller which shows more foliage, and the young jack pine needles have the lowest reflectivity in the red band (R_T^{RED} = 0.05) among the four sites and at the same time the highest NIR reflectivity (R_T^{NIR} = 0.53), resulting in a largest NDVI (0.83) for the sunlit foliage. For the shaded foliage, the NDVI increase to 0.95. The small contrast between sunlit and shaded foliage reflectivities can explain the symmetry about nadir observed by POLDER (Fig. 1). This effect of leaf optical properties is consistent with Fig. 6b which shows that changes in crown reflectivities induce systematic changes at all view zenith angles. The OA site differs from YJP mainly by its important understorey composed of hazelnut shrubs which increase the overall NDVI values compensating for slightly lower NDVI for the aspen leaves than the YJP needles. With the limited measurements, we cannot determine whether the differences found between the model and the measurements in Fig. 1 are caused by model deficiency or by measurement errors such as atmospheric corrections.

3.7. Main mechanisms controlling the NDVI for the four sites

With the simulation results shown in Figs. 6-10, we can now explain the mechanisms controlling the measured NDVI distributions in Fig. 1. The four scene components that compose the reflectances have different NDVI values that are determined by their red and NIR reflectivities. For all four sites, the largest scene component NDVI values are associated with the shaded components, and they are generally higher for the canopy than the background. Since the probabilities of seeing both shaded and sunlit crowns increase with view zenith angle, the NDVI values follow the same trend which results in a directional distribution of NDVI that is minimum at the hotspot where all the foliage and the ground scene components are illuminated, or at nadir where the maximum background can be seen, depending on the reflectivities and the scene proportions. NDVI variations near the hotspot can be seen more clearly in the simulations shown in Fig. 4 than those in Fig. 1 where the POLDER measurements were only available in large angular steps. It was shown that any changes in the gap fraction due to crown size, view angle, foliage density, etc., affects the NDVI, as more ground seen through the canopy generally decrease the NDVI.

Based on the reflectivities in Table. 1, the NDVI value for the shaded ground component in the OBS site is the largest among the four sites investigated because of the green moss and understory species. The OBS NDVI increases continuously from the hotspot to the nadir and to the large view zenith angles on the forward scattering side. This is mainly caused by the continuous increase in the probabilities of seeing the shaded crown. The elongated crowns at the OBS site cause the canopy gap fraction to decrease rapidly from the nadir. This is one explanation of the steeper change in the NDVI value with the VZA than the other sites where crowns are larger and the gap fraction varies less with the VZA. In OBS, the lowest NDVI at large backscattering VZAs is associated with the lowest NDVI for the sunlit crown (0.65) among the four species. On the forward scattering side at VZAs larger than 55°, the modelled NDVI in OBS (Fig. 4) shows a decreasing trend because of the cone and cylinder geometry. At large zenith angles, the cylindrical part of the crown is obscured and the scene is occupied mostly by the conical part. Because of the conical geometry, a small sunlit surface can be seen from the shaded side combined with a high red foliage reflectivity causes a decrease in the NDVI value. However, this trend is not found in the measurements because of the limited view angle range. The OBS site has the largest LAI (Table 1) but because the foliage is concentrated in dense pencil-like narrow crowns, the resulting NDVI is not the largest.

The low NDVI in OJP is caused by a combination of three factors: (i) a low tree density (1850 stems per hectare); (ii) a small LAI (2.2); and (iii) the lowest sunlit ground NDVI among the species studied. Both (i) and (ii) result in large canopy gap fractions. Near the vertical view direction, about half of the exposed ground in OJP is illuminated at SZA = 35°, resulting in the lowest NDVI among the four forest stands.

The YJP and OA sites have the highest NDVI among the four sites studied within the principal solar plane. The large NDVI in YJP can be explained by the reflectivities of the scene components (see Table 1).

The YJP site has a low LAI but with a larger crown size, hence the gap fraction is smaller which shows more foliage, and the young jack pine needles have the lowest reflectivity in the red band (= 0.05) among the four sites and at the same time the highest NIR reflectivity (= 0.53), resulting in a largest NDVI (0.83) for the sunlit foliage. For the shaded foliage, the NDVI increase to 0.95. The small contrast between sunlit and shaded foliage reflectivities can explain the symmetry

about nadir observed by POLDER (Fig. 1). This effect of leaf optical properties is consistent with Fig. 6b which shows that changes in crown reflectivities induce systematic changes at all view zenith angles. The OA site differs from YJP mainly by its important understorey composed of hazelnut shrubs, which increase the overall NDVI values compensating for slightly lower NDVI for the aspen leaves than the YJP needles.
With the limited measurements, we cannot determine whether the differences found between the model and the measurements in Fig. 1 are caused by model deficiency or by measurement errors such as atmospheric corrections.

4. Implications of NDVI directionality on derivation and validation of remote sensing products

NDVI of forest canopies is highly dependent on the difference in the directional distribution of reflectance between red and NIR bands. It has been shown that the NDVI directionality is pronounced in all four forests investigated. Numerical experiments indicate that the directionality results from various canopy optical and architectural attributes. For a sound validation of high-level remote sensing products such as LAI, the intermediate variables including reflectance and vegetation index, if used for deriving remote sensing products, should be validated as prerequisites. Errors in the surface reflectances are contagious for vegetation index and higher-level products, even though some of these errors are reduced by taking the ratio between the two bands. When the NDVI is validated at one combination of illumination and view geometries, its values in other combinations are not automatically known without the knowledge of the optical and structural properties of the stand and need to be further validated.
NDVI values derived from individual bands after BRDF corrections (Chen and Cihlar, 1997; Cihlar et al., 1997; Deering et al., 1990; Roujean et al., 1992; Walthall et al., 1985) are an improvement over non-corrected NDVI values. The BRDF correction algorithms are strongly cover type dependent. This is also evident from the model results and measurements shown in this paper. When possible, a stratification of the image by land cover type should be made. This is important because the NDVI directionality and magnitude are different among stands of different species investigated (Figs. 1 and 4; Deering et al., 1995). To further improve parameter retrieval, a stratification by age or stand density can also be considered. To ensure unbiased derivation of parameters within a remote sensing image or between multiple images, we also need to calculate reflectances of each pixel at a common illumination and view geometry. This can be done by constructing the directional distributions of reflectances for each cover type through empirical or semi-empirical fits (Wanner et al., 1995) to available data or through mechanistic modelling (e.g., using the 4-Scale model). The optimal choice of the geometry would be the vertical view and a representative solar zenith angle for the geographical area of concern, such as 45° for Canada (Cihlar et al., 1997). In using the NDVI for biophysical parameter mapping, it is evident from the simulation results that precautions should be taken for many canopy architectural attributes which affect the relationship between the NDVI and the parameter of interest. In addition to the effects of the background of variable understoreys, one should also be concerned with the spatial distribution pattern of the foliage. In forest stands, the distribution is controlled by the stand density and the spatial distribution pattern of trees. While the variations of these properties between large pixels may be small for natural stands, the variations between small pixels present a challenge for high resolution mapping of biophysical parameters. This problem deserves more attention in high spatial resolution (i.e., 100~102 m) remote sensing and

its product validation. Some attempts have been made to use textural parameters in high resolution airborne images for improving LAI estimation (Wulder et al., 1996).
The complexity in the NDVI-LAI relationship indicates strong limitations to the use of vegetation indices for LAI mapping. Inversion models may be used instead of vegetation indices (Gao and Lesht, 1997; Hall et al., 1995; Kuusk, 1991; Privette et al., 1996). However, inversion models also have to confront the same complexity and unknown canopy architectural attributes. When accurate multiple angle measurements for the same location are available, the directionality of NDVI may be used to improve LAI derivation rather than being treated as noise.

5. Summary

NDVI angular variations are found to be considerable in both limited measurements and in comprehensive model simulations. These variations cannot be ignored in the generation and validation of remote sensing products. Many canopy optical and geometrical attributes affect the directionality of the NDVI. For a given forest type with the same background, the spatial distribution patterns of foliage have pronounced effects on NDVI directionality. The most important geometrical attributes are the stand density and the tree distribution patterns. For the black spruce species predominant at high latitudes, sub-canopy architecture such as the geometry of branches and shoots has secondary but significant effects on the NDVI angular signature. These effects are much more pronounced for jack pine. As other vegetation indices (e.g., SR and MSR) can be derived from NDVI without additional information, their directionality should follow that of NDVI found in this study. In developing algorithms for deriving biophysical parameters using NDVI or other vegetation indices, it would be useful to stratify against not only the species but also the age and density because of the changes in the optical and structural properties.

References

Badhwar, G.D., R.B. MacDonald and N.C. Mehta, 1986. "Satellite-derived leaf-area-index and vegetation maps as input to global carbon cycle models--a hierarchical approach." Int. J. Remote Sensing, vol. 7, pp. 265-281.

Bréon, F.M., V. Vanderbilt, M. Leroy, P. Bicheron, C. L. Walthall and J.E. Kalshoven, 1996. "Evidence of Hot-spot Signature from Airborne POLDER Measurements." IEEE Trans. Geosc. Rem. Sens. vol 35, pp. 479- 484

Chen J.M., 1996a. "Evaluation of Vegetation Indices and Modified Simple Ratio for Boreal Applications." Canadian Journal of Remote Sensing, vol. 22, pp. 229-242.

Chen J.M. 1996b "Canopy Architecture and Remote Sensing of the Fraction of Photosyntheticaly Active Radiation Absorbed by Boreal Conifer Forests." IEEE Trans. Geosci. Rem. Sens., vol. 34, pp. 1353-1368.

Chen J.M. and T.A. Black, 1991. "Measuring Leaf Area Index of Plant Canopies with Branch Architecture." Agric. For. Meteorol., vol. 57, pp. 1-12.

Chen J.M., P.D. Blanken, T.A. Black, M. Guilbeault, and S. Chen, 1997. "Radiation Regime and Canopy Architecture in Boreal Aspen Forest." Agric. For. Meteorol. vol. 86, pp.107-125.

Chen J.M. and J. Cihlar 1996. "Retrieving Leaf Area Index of Boreal Conifer Forests using Landsat TM Images." Remote Sens. Environ. vol.55, pp. 153-162.

Chen J.M. and J. Cihlar 1997. "A Hotspot Function in a Simple Bidirectional Reflectance Model for Satellite Applications" J. Geophys. Res. vol. 102, No. D22, pp. 25,907-15,913.

Chen J.M. and S. G. Leblanc, 1997. "A Four-Scale Bidirectional Reflectance Model Based on Canopy Architecture." IEEE Trans. Geosci. Rem. Sens., vol. 35, pp. 1316-1337

Cihlar, J., H. Ly, Z. Li, J. Chen, H. Pokrant, and F. Huang, 1997. "Multitemporal, Multichannel AVHRR Data Sets for Land Biosphere Studies: Artifacts and Corrections." Remote Sens. Environ. vol. 60, pp. 35-57

Deering D.W., T.F. Eck, and J. Otterman. "Bidirectional Reflectance Model of the Earth's Surfaces and their Three-Parameter Soil Characterization." Agri. For. Meteorol. vol. 52, pp. 71-93.

Deering D.W., E.M. Middleton and T.F. Eck, 1994. "Reflectance Anisotropy for a Spruce-Hemlock Forest Canopy." Remote Sens. Environ. vol. 47, pp. 242-260.

Deering D.W., S.P. Ahmad, and T.F. Eck 1995. "Temporal Attributes of the Bidirectional Reflectance for Three Boreal Forest Canopies." Proc. Int'l Geosci. Remote Sensing Symposium, pp. 1239-1241.

Deschamps P-Y, F. M. Bréon, M. Leroy, A. Podaire, A. Bricaud, J-C Buriez and G. Sève 1994. "The POLDER Mission: Instrumental Characteristic and Scientific Objectives." IEEE Trans. Geosci. Rem. Sens., vol. 32, pp. 598-613.

Fassnacht, K.S., S.T. Gower, M.D. MacKenzie, E.V. Nordheim, and T.M. Lillesand, 1997. "Estimating the Leaf Area Index of North Central Wisconsin Forest Using the Landsat Thematic Mapper." Remote Sens. Environ. vol. 61, pp. 229-245.

Franklin, J., J. Michaelsen, and A.H. Strahler, 1985. "Spatial Analysis of Density Dependent Pattern in Coniferous Forest Stands." Vegetatio, vol. 64, pp.29-36.

Gao, W. and B.M. Lesht, 1997. "Model Inversion of Satellite-Measured Reflectance for Obtaining Surface Biophysical and Bidirectional Reflectance Characteristics of Grassland." Remote Sens. Environ. vol. 59, pp. 461-471.

Goel N.S. and W. Qin, 1994, "Influence of Canopy Architecture on Relationships Between Various Vegetation Indices and LAI and FPAR: a Computer Simulation." Remote Sens. Environ., vol. 10, pp. 309-347

Goward, S.N. and K.E. Huemmrich, 1992. "Vegetation Canopy PAR Absorbance and the Normalized Difference Vegetation Index: an Assessment using the SAIL Model". Remote Sens. Environ. vol. 39, pp. 119-140.

Gutman, G.G., 1991. "Vegetation Indices from AVHRR: An Update and Future Prospects." Remote Sens. Environ., vol. 35, pp. 121-136.

Hall, F.G., Y.E. Shimabukuro, and K.F. Huemmrich. 1995. "Remote Sensing of Forest Biophysical Structure Using Mixture Decomposition and Geometric Reflectance Models." Ecological Applications, vol. 5, pp. 993-1013.

Hapke, B., D. DiMucci, R. Nelson and W. Smythe, 1996. "The Cause of the Hot Spot in Vegetation Canopies and Soils: Shadow-Hiding Versus Coherent Backscatter." Remote Sens. Environ., vol. 58, pp. 63-68.

Huete, A.R. 1988. "A Soil Adjusted Vegetation Index (SAVI)," Remote Sens. Environ., vol. 25, pp. 295-309

Huemmrich K.F. and S.N. Goward, 1997. "Vegetation Canopy PAR Absorbance and NDVI: An Assessment for Ten Tree Species with the SAIL Model." Remote Sens. Environ., vol. 61, pp. 254-269.

Kuusk, A., 1991. "Determination of Vegetation Canopy Parameters from Optical Measurements." Remote Sen. Environ. vol. 37, pp. 207-218.

Landry R., R.A. Fournier, F.J. Ahern and R.H. Lang, 1997. "Tree Vectorization: A methodology to Characterize Fine Tree Architecture in Support of Remote Sensing Models." Canadian Journal of Remote Sensing, vol. 23, pp. 91-107.

Leblanc S.G., P. Bicheron, J.M. Chen, M. Leroy and J. Cihlar, 1999. "Investigation of Directional Reflectance in Boreal Forests with an Improved 4-Scale Model and Airborne POLDER Data." Submitted to IEEE Trans. Geosci. Rem. Sens. vol. 37 No. 3 pp.1396-1414.

Li, X. and A.H. Strahler, 1992. "Geometric-Optical Bidirectional Reflectance Modeling of the Discrete Crown Vegetation Canopy: Effect of Crown Shape and Mutual Shadowing.", IEEE Trans. Geosci. Rem. Sens., vol. 30, pp. 276-292.

Middleton, E., 1991. "Solar Zenith Angle Effects on Vegetation Indices in Tallgrass Prairie." Remote Sens. Environ., vol. 38, pp. 45-62.

Middleton, E., S.S. Chan, R.J. Rusin and S.K. Mitchell, 1997 "Optical Properties of Black Spruce and Jack Pine Needles at BOREAS sites in Saskatchewan, Canada." Canadian Journal of Remote Sensing, vol. 23, pp. 108-129.

Moreau, L. and Z. Li, 1996. "A new Approach for Remote Sensing of Canopy absorbed Photosynthetically Active Radiation. Part 2: A Radiative Transfert Simulation Study in Canopies." Remote Sens. Environ., vol. 55, pp. 192-204.

Myneni, R.B. and J. Ross (Eds.), 1991. "Photon-Vegetation Interaction." Sprigler-Verlag. 565

Myneni, R.B. and D. L. Williams, 1994. "On the Relationship Between FAPAR and NDVI." Remote Sens. Environ., vol. 49, pp. 200-211

Neyman, J., 1939. "On a New Class of 'Contagious' Distribution Applicable in Entomology and Bacteriology", Annals of Mathematical Statistics, vol. 10, pp. 35-57.

Nilson T. and U. Peterson, 1991. "A Forest Canopy Reflectance Model and a Test Case." Remote Sens. Environ., vol. 37, pp. 131-142.

Peterson, D.L., M.A. Spanner, S.W. Running, and K.B. Teuber, 1987. "Relationship of Thematic Mapper Simulator Data to Leaf Area Index of Temperate Coniferous Forests." Remote Sens. Environ., vol. 22, pp. 323-341.

Pinter, P.J. Jr., 1993, "Solar Angle Independence in the Relationship Between Absorbed PAR and Remotely Sensed Data for Alfafa." Remote Sens. Environ. vol. 46, pp. 19-25

Privette, J.L., W.J. Emery and D.S. Schimel, 1996. "Inversion of a Vegetation Reflectance Model with NOAA AVHRR Data." Remote Sens. Environ., vol. 58, pp. 187-200.

Rosema, A, W. Verhoef, H. Noorbergen, and J.J. Borgesius, 1992. "A New Forest Light Interaction Model in Support of Forest Monitoring." Remote Sens. Environ. vol. 42, pp. 23-41.

Roujean, J-L, M. J. Leroy, and P.-Y. Deschamps. "A Bidirectional Reflectance Model of the Earth's Surface for the Correction of Remote Sensing data." J. Geophys. Res. vol. 97, 20, pp. 20,455-20,468.

Rouse J.W., R.W. Hass, J.A. Shell and D.W. Deering, 1974. "Monitoring Vegetation Systems in the Great Plains with ERTS-1." Third Earth Resources Technology Satellite Symposium. vol. 1, pp. 309-317.

Sellers, P., F. Hall, H. Margolis, B. Kelly, D. Baldocchi, D. Den Hartog, J. Cihlar, M. Ryan, B. Goodison, P. Crill, J. Ranson, D. Lettermaier and D. E. Wickland, 1991. "BOREAS-Boreal Ecosystem-Atmosphere Study: Global Change Biosphere Atmosphere Interactions in the Boreal Forests Biome-Science Plan." no. 923, NASA/GSFC, Greenbelt, MD, pp. 67.

Sellers, P.J., S.O. Los, C.J. Tucker, C.O. Justice, D.A. Dazlich, G.J. Collatz, and D.A. Randall, 1995. "A global 1°*1° NDVI data set for climate studies. Part 2: The generation of Global Fields of Terrestrial Biophysical Parameters from the NDVI", Int. J. Remote Sensing, vol. 15, pp. 3519-3545

Sinhg, S.M., 1988. "Simulation of Solar Zenith Angle Effect on Global Vegetation Index (GVI) Data." Int. J. Remote Sens., vol. 9, pp.237-248.

Spanner M.A, L.L Pierce, S.W. Running, and D. L. Peterson, 1990. "The Seasonality of AVHRR Data of Temperate Coniferous Forests: Relationship with Leaf Area Index", Remote Sens. Environ., vol. 33, pp. 97-112.

Teillet P. M., K. Staenz, and D. J. Williams, 1997. "Effects of Spectral, Spatial, and Radiometric Characteristics on Remote Sensing Vegetation Indice of Forested Regions." Remote Sens. Environ. vol. 61, pp. 139-149.

Verhoef, W, 1984. "Light Scattering by Leaf Layers with Application to Canopy Reflectance Modelling: The Sail Model." Remote Sens. Environ., vol. 16, pp. 125-141.

Vermote, E.D., J.L. Deuze, and J.J. Morcrette. 1996 "Second Simulation of the Satellite Signal in the Solar Spectrum: an overview". IEEE Trans. Geosci. Rem. Sens., vol. 35, pp. 675-686.

Walthall, C.L., J.M. Norman, J.M. Welles, G. Campbell, and B.L. Blad. 1995 "Simple Equation to Approximate the Bidirectional Reflectance from Vegetation Canopies and Bare Soil Surface." Appl. Opt., vol. 24, pp. 383-387.

Wanner, W, X. Li, and A.H. Strahler, 1995. "On the derivation of Kernel-Driven Models of Bidirectional Reflectance." J. Geophys. Res. Vol 100, No. D10, pp. 21,077-21,089.

White, H.P., J.R. Miller, J.M. Chen, D.R. Peddle and G. McDermid, 1995. "Seasonal Change in Mean Understory Reflectance for Boreal Site: Preliminary Results", Proc. 17th Canadian Symposium on Remote Sensing.

Wulder, M.A., S.E. Franklin and M.B. Lavigne, 1996. "High Spatial Resolution Optical Image Texture for Improved Estimation of Forest Stand Leaf Are Index." Canadian Journal of Remote Sensing, vol. 22, pp. 441-449.

Noted errors from the version published in the Canadian Journal of Remote Sensing.

S. G. Leblanc, J. M. Chen and J. Cihlar,
Directionality of NDVI in Boreal Forest: A Model Simulation of Measurements"
Canadian Journal Remote Sensing, Vol. 23, No. 4,
December 1997, pp. 369-380.
On page 375, some of the shaded reflectivities miss "Z" in the subscripts.